



# Direct growth of Ge<sub>1-x</sub>Sn<sub>x</sub> films on Si using a cold-wall ultra-high vacuum chemical-vapor-deposition system

Aboozar Mosleh<sup>1,2\*</sup>, Murtadha A. Alher<sup>2,3</sup>, Larry C. Cousar<sup>1,4</sup>, Wei Du<sup>2</sup>, Seyed Amir Ghetmiri<sup>1,2</sup>, Thach Pham<sup>2</sup>, Joshua M. Grant<sup>5</sup>, Greg Sun<sup>6</sup>, Richard A. Soref<sup>6</sup>, Baohua Li<sup>4</sup>, Hameed A. Naseem<sup>2</sup> and Shui-Qing Yu<sup>2</sup>

<sup>1</sup> Microelectronics-Photonics Graduate Program ( $\mu$ EP), University of Arkansas, Fayetteville, AR, USA

<sup>2</sup> Department of Electrical Engineering, University of Arkansas, Fayetteville, AR, USA

<sup>3</sup> Mechanical Engineering Department, University of Karbala, Karbala, Iraq

<sup>4</sup> Arktonics, LLC, Fayetteville, AR, USA

<sup>5</sup> Engineering-Physics Department, Southern Arkansas University, Magnolia, AR, USA

<sup>6</sup> Department of Engineering, University of Massachusetts Boston, Boston, MA, USA

## Edited by:

Jifeng Liu, Dartmouth College, USA

## Reviewed by:

Fabio Iacona, National Research Council, Italy

Christophe Labbé, Ecole Nationale Supérieure d'Ingénieurs de Caen, France

## \*Correspondence:

Aboozar Mosleh, Engineering Research Center (ENRC), 700 Research Center Boulevard, Fayetteville, AR 72701, USA  
e-mail: amosleh@gmail.com

Germanium–tin alloys were grown directly on Si substrate at low temperatures using a cold-wall ultra-high vacuum chemical-vapor-deposition system. Epitaxial growth was achieved by adopting commercial gas precursors of germane and stannic chloride without any carrier gases. The X-ray diffraction analysis showed the incorporation of Sn and that the Ge<sub>1-x</sub>Sn<sub>x</sub> films are fully epitaxial and strain relaxed. Tin incorporation in the Ge matrix was found to vary from 1 to 7%. The scanning electron microscopy images and energy-dispersive X-ray spectra maps show uniform Sn incorporation and continuous film growth. Investigation of deposition parameters shows that at high flow rates of stannic chloride the films were etched due to the production of HCl. The photoluminescence study shows the reduction of band-gap from 0.8 to 0.55 eV as a result of Sn incorporation.

**Keywords:** chemical-vapor-deposition, Si photonics, Ge alloys, photoluminescence, Ge–Sn

## INTRODUCTION

The discovery and development of Ge<sub>1-x</sub>Sn<sub>x</sub> epitaxy technology has enabled silicon photonics to be explored in a different scope of a material platform. The ability of band-gap engineering by varying Sn mole fraction, along with its compatibility to the complementary metal–oxide–semiconductor (CMOS) process, has paved the way for highly competitive Si-based near and mid-infrared optoelectronic devices. Recent reports on the fabrication and characterization of high performance Ge<sub>1-x</sub>Sn<sub>x</sub> devices such as modulators (Kouvetakis et al., 2005), photodetectors (Conley et al., 2014a,b), and light emitting diodes (LEDs) (Du et al., 2014a) show great potential for Ge<sub>1-x</sub>Sn<sub>x</sub> being adopted by industry in the near future. Cutting-edge reports on Ge<sub>1-x</sub>Sn<sub>x</sub>, achieving a direct band-gap group IV alloy (Du et al., 2014b; Ghetmiri et al., 2014a; Li et al., 2014; Wirths et al., 2014), is a turning point for the technology to be pursued for the demonstration of an efficient group IV laser. In addition, due to the tunable lattice constant and formation of Lomer dislocations, Ge<sub>1-x</sub>Sn<sub>x</sub> has been shown to work as a universal compliant buffer layer to grow high quality lattice mismatched materials, like III–Vs, on Si (Beeler et al., 2011a; Mosleh et al., 2014).

A variety of challenges exist for the growth of Ge<sub>1-x</sub>Sn<sub>x</sub> alloys on Si such as large lattice mismatch between Ge<sub>1-x</sub>Sn<sub>x</sub> and Si (more than 4.2%), low solid solubility of Sn in Ge (less than 0.5%), and instability of diamond lattice Sn ( $\alpha$ -Sn) above 13°C. Therefore, growth can only possibly be done under non-equilibrium conditions. Different growth methods have been demonstrated for Ge<sub>1-x</sub>Sn<sub>x</sub> growth in which molecular beam epitaxy (MBE) and chemical-vapor-deposition (CVD) have obtained device quality material and high Sn incorporation. For the MBE method,

both gas source and solid source MBE have been used by different groups to grow Ge<sub>1-x</sub>Sn<sub>x</sub> films (Gurdal et al., 1998; Takeuchi et al., 2007; Chen et al., 2011; Werner et al., 2011; Stefanov et al., 2012; Bhargava et al., 2013; Oehme et al., 2013; Wang et al., 2013).

The other parallel approach of Ge<sub>1-x</sub>Sn<sub>x</sub> growth is CVD. The early results of CVD growth by Kouvetakis and Chizmeshya (2007) at Arizona State University (ASU) showed the ability to grow Ge<sub>1-x</sub>Sn<sub>x</sub> film directly on Si using a hot-wall ultra-high vacuum CVD (UHV-CVD) system with deuterated Stannane (SnD<sub>4</sub>) as the Sn precursor along with different chemistries of germanium. Due to the high cost and instability of SnD<sub>4</sub>, other precursors such as tetramethyl tin [Sn(CH<sub>3</sub>)<sub>4</sub>] and stannic chloride (SnCl<sub>4</sub>) have been explored to grow Ge<sub>1-x</sub>Sn<sub>x</sub> alloys. Vincent et al. (2011) (from IMEC using atmospheric pressure CVD) and Kim et al. (Chen et al., 2013) [from Applied Materials/Stanford University using reduced pressure-CVD (RP-CVD)] have reported successful growth of Ge<sub>1-x</sub>Sn<sub>x</sub> by using SnCl<sub>4</sub> and a high cost Ge precursor digermane (Ge<sub>2</sub>H<sub>6</sub>) and carrier gases on a Ge-buffered Si substrate. Using the same SnCl<sub>4</sub> and Ge<sub>2</sub>H<sub>6</sub> precursors and carrier gases, Mantl et al. (Wirths et al., 2013) (from PGI9-IT) demonstrated direct growth of Ge<sub>1-x</sub>Sn<sub>x</sub> on Si using showerhead technology in an RP-CVD chamber. In the recent report, Tolle et al. (Margetis et al., 2014; Mosleh et al., 2014a) (ASM company) have achieved Ge<sub>1-x</sub>Sn<sub>x</sub> growth using an industry prevail RP-CVD reactor in collaboration with University of Arkansas (UA). Low-cost Germane (GeH<sub>4</sub>) and SnCl<sub>4</sub> with carrier gases of N<sub>2</sub>/H<sub>2</sub> were used to grow Ge<sub>1-x</sub>Sn<sub>x</sub>. A Ge buffer was deposited between the Si substrate and the Ge<sub>1-x</sub>Sn<sub>x</sub> layer in order to compensate the lattice mismatch between the layers. **Table 1** lists the different research groups that have grown Ge<sub>1-x</sub>Sn<sub>x</sub> using CVD. Different

**Table 1 | A summary of reports on Ge<sub>1-x</sub>Sn<sub>x</sub> growth using CVD methods by different research groups.**

Growth team	Deposition system	Deposition gas precursors				Carrier gas	Buffer layer
		Ge	Cost	Sn	Cost		
ASU (Kouvetakis and Chizmeshya, 2007)	UHV-CVD	Different chemistries	High	SnD <sub>4</sub>	High	Yes	No
IMEC (Vincent et al., 2011)	AP-CVD	Ge <sub>2</sub> H <sub>6</sub>	High	SnCl <sub>4</sub>	Low	Yes	Ge
Applied materials (Chen et al., 2013)	RP-CVD	Ge <sub>2</sub> H <sub>6</sub>	High	SnCl <sub>4</sub>	Low	Yes	Ge
PGI9-IT (Wirths et al., 2013)	RP-CVD	Ge <sub>2</sub> H <sub>6</sub>	High	SnCl <sub>4</sub>	Low	Yes	No
ASM/UA (Margetis et al., 2014; Mosleh et al., 2014a)	RP-CVD	GeH <sub>4</sub>	Low	SnCl <sub>4</sub>	Low	Yes	Ge
UA (this work)	UHV-CVD	GeH <sub>4</sub>	Low	SnCl <sub>4</sub>	Low	No	No

growth methods and the cost effectiveness of the gas precursors are compared.

In this paper, we report direct growth of strain-relaxed Ge<sub>1-x</sub>Sn<sub>x</sub> films on Si substrates with Sn mole fractions up to 7% using a cold-wall UHV-CVD system. Stannic chloride and germane were chosen as the precursors which are low-cost and commercially available. The growth of Ge<sub>1-x</sub>Sn<sub>x</sub> films was achieved without using any carrier gases and buffer layers. In order to investigate the material quality, the X-ray diffraction (XRD), high-resolution transmission electron microscopy (TEM), energy-dispersive X-ray spectroscopy (EDX), Raman spectroscopy, and photoluminescence (PL) measurements have been conducted.

## EXPERIMENT

### GROWTH METHOD

A cold-wall UHV-CVD system was adopted to grow Ge<sub>1-x</sub>Sn<sub>x</sub> films (see **Figure 1** for machine schematic). The system composes a load-lock chamber with a base pressure of 10<sup>-6</sup> Pa and a process chamber whose base pressure reaches 10<sup>-8</sup> Pa using the turbo-molecular and cryogenic pumps, respectively. Due to low-temperature growth of the films, removal of oxygen and water vapor is critical which was achieved by using a cryogenic pump. The turbo-molecular pumps are backed by mechanical pumps. The heating stage consisted of a pyrolytic graphite heater with a thermocouple placed at the same distance away from the heater as the wafer. The sample holder rotates up to 80 rpm for uniform film growth. The gas flow is through a side entry port, controlled by mass flow controllers (MFCs). Stannic chloride is a volatile liquid with vapor pressure of 2.4 kPa at one atmospheric pressure. Therefore, the evaporation could produce enough pressure to be passed through the MFC.

Germanium–tin films were grown on 4'' (001) p-type Si substrates with 5–10 Ω cm resistivity. Prior to loading the samples, they were cleaned in a two-step process: (1) Piranha etch solution [H<sub>2</sub>SO<sub>4</sub>:H<sub>2</sub>O<sub>2</sub> (1:1)], (2) oxide strip HF dipping [H<sub>2</sub>O:HF (10:1) using 48% pure HF] followed by nitrogen blow drying. The final oxide strip step was not followed by a water rinse as it reduces the life-time of hydrogen passivation and exposes the surface to ambient oxygen (Mosleh et al., 2013, 2014b). The experiments were carried out at reduced pressures of 13, 40, 65, 95, 130, 200, and 260 Pa and at temperatures as low as 300°C. Germane (GeH<sub>4</sub>) and stannic chloride (SnCl<sub>4</sub>) were used as the precursors for Ge<sub>1-x</sub>Sn<sub>x</sub> growth. The gas flow ratio (GeH<sub>4</sub>/SnCl<sub>4</sub>) was set to 5, 3.3, 2.5, and 1.6. Depending on the growth parameters such as gas flow

ratio and deposition pressure, a growth rate of 20–3.3 nm/min was achieved.

### CHARACTERIZATION METHOD

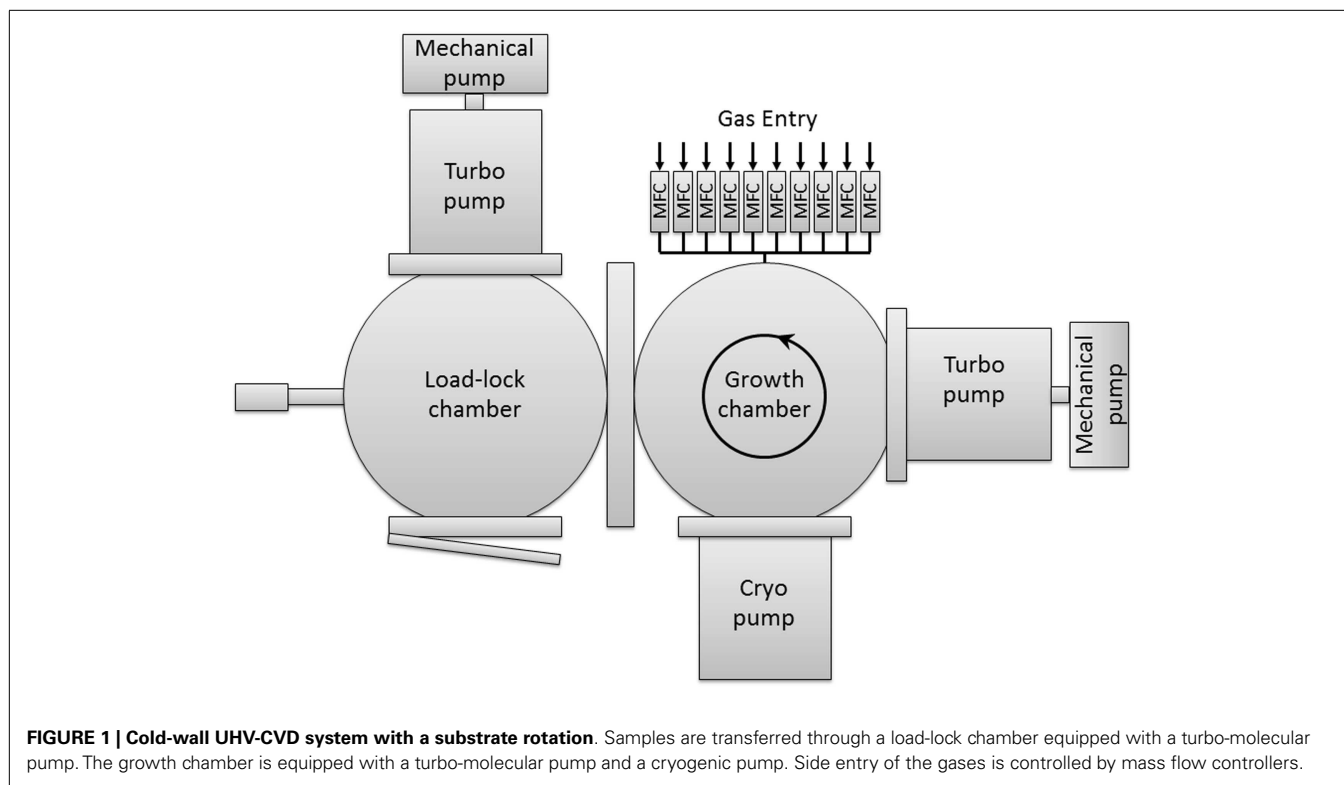
Analysis of Sn mole fraction, lattice constant, growth quality, and strain in the Ge<sub>1-x</sub>Sn<sub>x</sub> films were conducted using a high-resolution X-ray diffractometer. High-resolution TEM (TITAN) with an accelerating voltage of 300 kV was used to investigate crystal orientation and defects in the grown epi-layers as well as determining the thicknesses of the samples. Surface morphology of the samples was investigated by a scanning electron microscope equipped with EDX. Room temperature PL measurements were carried out using a 690-nm excitation laser. The PL signal was collected by a grating-based spectrometer equipped with a thermoelectric-cooled PbS detector (cut-off at 3 μm) for spectral analysis.

## RESULTS AND DISCUSSION

### MATERIAL CHARACTERIZATION

The 2θ-ω XRD scan was performed from the symmetric (004) plane to obtain the out-of-plane lattice constant of the Ge<sub>1-x</sub>Sn<sub>x</sub> films. **Figure 2A** shows the peak at 69° corresponding to a satisfaction of the Bragg condition by Si (001) substrate, and the peaks at lower angles of 66–65° due to larger lattice size of the Ge<sub>1-x</sub>Sn<sub>x</sub> layers. The difference in the position of Ge<sub>1-x</sub>Sn<sub>x</sub> peaks is due to the difference in the Sn mole fractions of Ge<sub>1-x</sub>Sn<sub>x</sub> layers. Different compositions were achieved from 1 to 7% with desirable crystal quality. The Ge<sub>1-x</sub>Sn<sub>x</sub> peaks are broadened for two reasons: (1) thin film thickness of the layers and (2) presence of mosaicity in the Ge–Sn crystal and formation of defects as a result of strain relaxation. The full width at half maximum (FWHM) of the Ge<sub>1-x</sub>Sn<sub>x</sub> peaks are between 0.28 for 1% Sn film and 0.36 for 7% Sn film. The change in FWHM depends on various factors such as film thickness, relaxation, and quality and there is no trend showing that the FWHM of the peaks change as the Sn composition increases.

In order to calculate the total lattice constant and the strain in the film, an asymmetric reciprocal space mapping (RSM) from (–2, –2, 4) plane was performed. The RSM scans provide measurement of the in-plane (*a*<sub>||</sub>) and out-of-plane (*a*<sub>⊥</sub>) lattice constant of Ge<sub>1-x</sub>Sn<sub>x</sub> alloys. The total lattice constant *a*<sub>0</sub><sup>GeSn</sup> was calculated by taking into account the elastic constants of Ge<sub>1-x</sub>Sn<sub>x</sub> (Beeler et al., 2011b). Knowing the total lattice constant, the Sn mole fractions is calculated through Vegard's law with the bowing factor of *b* = 0.0166 Å (Moontragoon et al., 2012). **Figure 2B**



shows the RSM of 6% Sn sample. The  $x$ -axis shows  $Q_z$  in reciprocal lattice unit (rlu) which is related to the out-of-plane lattice constant ( $L$ ) and the  $y$ -axis shows  $Q_x$  which is related to the in-plane lattice constant ( $H$  or  $K$ ). Direction of the spread in the  $\text{Ge}_{0.94}\text{Sn}_{0.06}$  peak does not show a compositional gradient in the sample because it is related to the relaxation of the lattice on Si substrate. Large lattice mismatch between Sn and Ge is the main reason for a large spread in the omega direction. The relaxation line in **Figure 2B** shows that the films which are grown above are tensile strained and the films grown underneath are compressively strained. The  $\text{Ge}_{0.94}\text{Sn}_{0.06}$  peak is observed to be on the relaxation line and the relaxation is measured to be 97%.

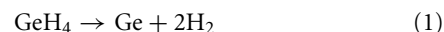
Calculation of total strain in other samples shows that all the films are more than 95% relaxed. **Table 2** shows the lattice constants of the  $\text{Ge}_{1-x}\text{Sn}_x$  alloys, their Sn mole fraction, and strain relaxation percentage.  $\text{Ge}_{1-x}\text{Sn}_x$  films were almost fully relaxed mainly due to large lattice mismatch between Si (5.431 Å) and  $\text{Ge}_{1-x}\text{Sn}_x$  (above 5.658 Å) and small critical thickness (Mosleh et al., 2014a). The other reason for relaxation of Ge (and similarly  $\text{Ge}_{1-x}\text{Sn}_x$ ) films on Si is the thermal mismatch between these two materials. High temperature growth (above 500°C) and rapid cool down has been the main method for achieving tensile strained Ge on Si (Conley et al., 2014a). The  $\text{Ge}_{1-x}\text{Sn}_x$  samples were grown at 300°C for 30 min and we have not achieved tensile strained films; however, the thermal mismatch between Si and  $\text{Ge}_{1-x}\text{Sn}_x$  has helped relaxing the compressive strain. The strain has been mainly relieved through formation of misfit dislocations including Lomer misfit dislocation. The cross-sectional TEM image in **Figure 2C** shows formation of such dislocations

at the  $\text{Ge}_{1-x}\text{Sn}_x/\text{Si}$  interface. In addition, **Figure 2B** shows that strain relaxation occurred by formation of misfit dislocations at the interface. The TEM image shows that the grown film was fully epitaxial. Film thickness of the samples is listed in **Table 2**.

The SEM scan/EDX spectra of the samples show surface morphology of the sample as well as Sn incorporation in the Ge matrix. The EDX spectra in **Figure 2D** show the presence of Ge, Si, and Sn in the  $\text{Ge}_{0.94}\text{Sn}_{0.06}$  film. Due to the high count collection of secondary electrons from the substrate, the ratio of Sn and Ge cannot exactly reveal the percentage of Sn in Ge. The presence of carbon and oxygen in the EDX spectra is mainly due to the contamination and oxidation of the film after exposure to ambient air. The EDX maps for Ge (**Figure 2E**) and Sn (**Figure 2F**) display uniform incorporation of Sn. The SEM image shows continuous growth of  $\text{Ge}_{1-x}\text{Sn}_x$  without observation of locally crystalline patches. No segregation and precipitation of Sn was observed on the films which indicates robust and stable growth of the films.

#### GROWTH MECHANISM

Growth of  $\text{Ge}_{1-x}\text{Sn}_x$  on a Si substrate requires considering the reaction of byproducts and reduction of activation energy by introducing carrier gases. Stannic chloride has a tendency to etch Ge due to the presence of chlorine in the chemistry of the molecule. The byproduct of  $\text{GeH}_4 + \text{SnCl}_4$  reaction is HCl which is an etchant gas for germanium and silicon (Bogumilowicz et al., 2005). Following reactions show different mechanisms of film deposition as well as HCl production in the chamber:



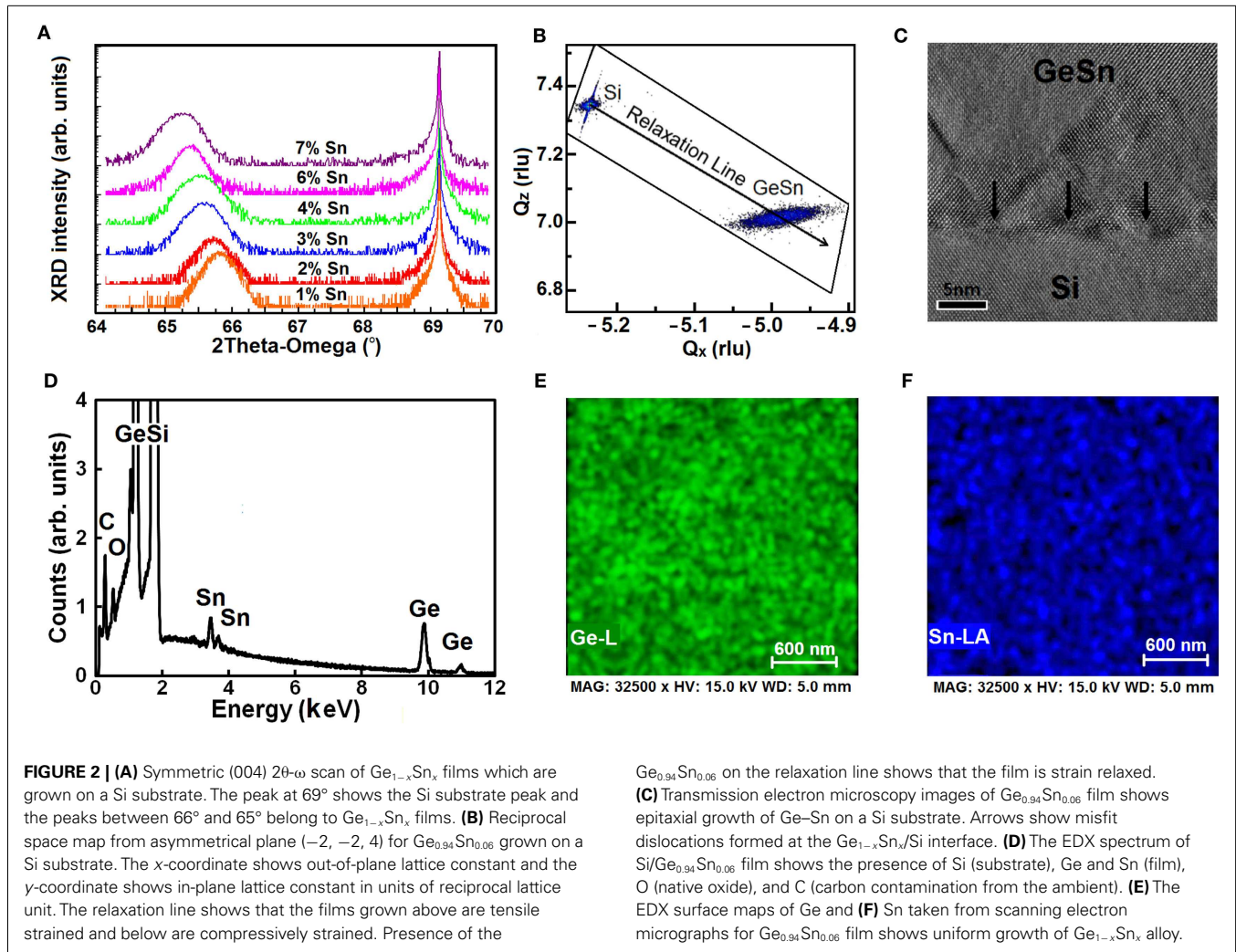
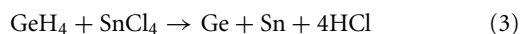
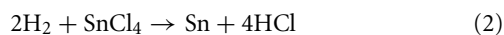


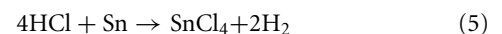
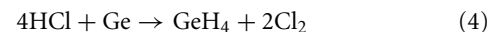
**Table 2 | Tin mole fraction calculation, lattice constant, and relaxation percentage of the grown samples.**

Sample no.	Sn (%)	$a_{\parallel}$ (nm)	$a_{\perp}$ (nm)	$a$ (nm)	Relaxation (%)	Thickness (nm)
1	1.2	5.666	5.671	5.668	98	615
2	2.1	5.673	5.679	5.676	98	423
3	2.9	5.678	5.687	5.682	97	295
4	4.2	5.689	5.695	5.692	98	207
5	5.8	5.699	5.712	5.706	97	108
6	7.0	5.715	5.719	5.717	99	532



Higher temperature of the substrate results in higher density of depositing ad-atoms (Ge and Sn); however, it will result in production of HCl at a higher rate. In addition, higher flow rate of  $\text{SnCl}_4$  increases the production rate of HCl as well. Controlling the temperature and flow rate of the gases could control the process

so that growth is the dominant process in the chamber. The Ge/Sn film will be etched by HCl through the following reactions:



Domination of etching over growth is the main mechanism that prevents direct growth of  $\text{Ge}_{1-x}\text{Sn}_x$  on Si.

By controlling the flow through MFCs, we have grown  $\text{Ge}_{1-x}\text{Sn}_x$  films on Si at different pressures with a fixed flow ratio of  $\text{GeH}_4/\text{SnCl}_4 = 1.6$ . Growth was observed at 13 Pa of deposition pressure and continued until the deposition pressure increased to 130 Pa. **Figure 3A** shows the thickness of  $\text{Ge}_{1-x}\text{Sn}_x$  films versus deposition pressure of the chamber as well as Sn incorporation percentage. Incorporation of Sn in the Ge lattice is increased by raising the pressure due to the higher residence time of the precursors in the chamber. The residence time of the gases has increased from 2 s at 13 Pa to 19 s at 130 Pa. Meanwhile, HCl etched more of the  $\text{Ge}_{1-x}\text{Sn}_x$  films after deposition at higher pressures. This trend has continued to 130 Pa and no growth has been observed at 200 and 265 Pa. The increase in Sn composition from 1 to 6%

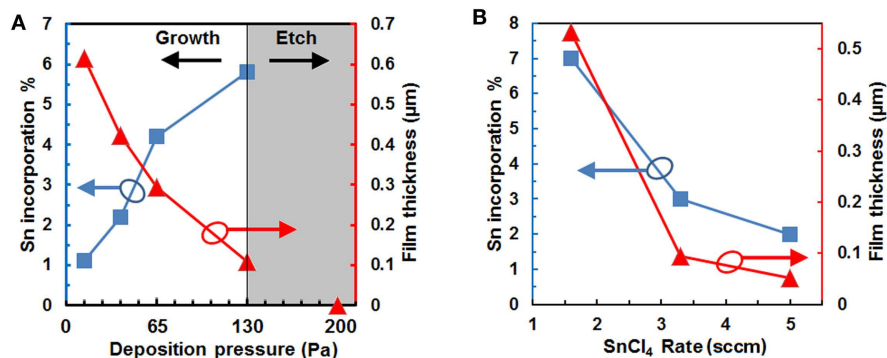


**FIGURE 3 | (A)** Variation of Sn incorporation percentage versus deposition pressure. Films were etched away for deposition pressures higher than 130 Pa. The secondary axis on the right shows the reduction of film thickness

as a result of increase in the deposition pressure. **(B)** Tin incorporation and film thickness of the samples grown at 65 Pa growth pressure versus  $\text{GeH}_4/\text{SnCl}_4$  flow ratios.

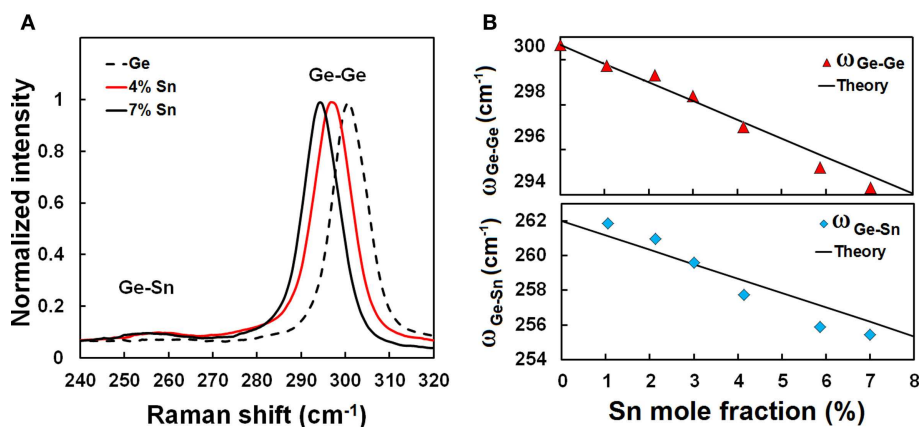


**FIGURE 4 | (A)** Raman spectra of the  $\text{Ge}_{1-x}\text{Sn}_x$  film grown on a Si substrate. The shift in the Ge–Ge peak is due to the incorporation of Sn in Ge lattice. The shoulder on the left side of the Ge–Ge peak is due to the Ge–Sn peak at  $285\text{ cm}^{-1}$ . The Ge–Sn peak is shown at lower wavenumber of  $250\text{--}260\text{ cm}^{-1}$ . **(B)** Ge–Ge and Ge–Sn peak shifts versus

Sn mole fraction. The solid symbols are experimental data and the curves are theoretical predictions for relaxed films. The Ge–Ge peak is expected to shift  $0.8310\text{ cm}^{-1}$  for every 1% Sn incorporation in relaxed films. The expected shift ( $0.8311\text{ cm}^{-1}$ ) for Ge–Sn peak is very close to that of Ge–Ge.

has been accompanied with reduction in the thickness from 615 to 108 nm. Films that were expected to have higher than 6% Sn content were totally etched off. Therefore, in order to grow higher Sn content films, growth mechanism under fixed pressure and changing the  $\text{SnCl}_4$  flow was studied. Higher film thickness and higher Sn incorporation was achieved as a result of domination of growth over etching. **Figure 3B** shows Sn incorporation in  $\text{Ge}_{1-x}\text{Sn}_x$  films versus  $\text{SnCl}_4$  flow rate at 95 Pa deposition pressure. The secondary axis of **Figure 3B** shows film thicknesses of the samples. Due to the dominance of etching for higher  $\text{SnCl}_4$  flow rate, the films were mostly etched and the film thickness was less than 100 nm.

Introduction of carrier gases has different effects on the growth of  $\text{Ge}_{1-x}\text{Sn}_x$  films. Hydrogen changes the balance in the reaction to produce more HCl. Consequently, the  $\text{GeH}_4/\text{SnCl}_4$  ratio at which the  $\text{Ge}_{1-x}\text{Sn}_x$  films were depositing will not result in growth when hydrogen is introduced in the chamber. In addition, introduction of nitrogen and argon as carrier gases will reduce the activation

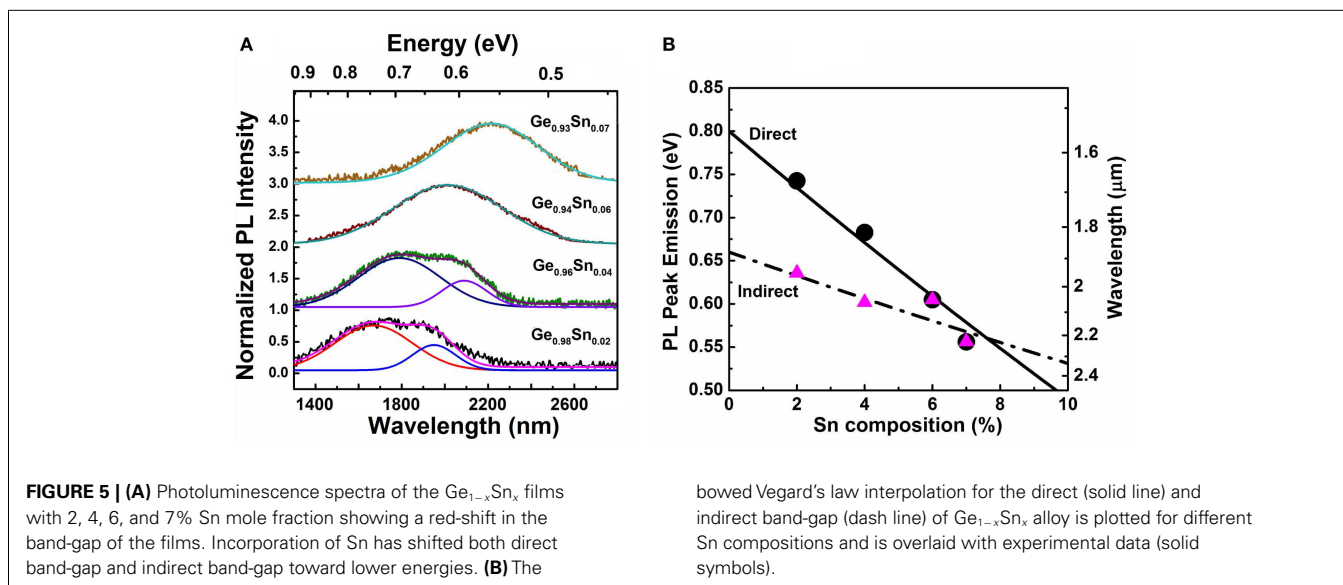
energy of the growth (Wirths et al., 2013). Although reduction of activation energy enables easier breakdown of the molecules on the surface and enhances the growth quality and growth rate, it would prepare the conditions for easier etch due to the presence of an etchant agent. Therefore, the presence of carrier gases pushes the competition between growth and etching toward etching, resulting in film etching at even lower flow rates of carrier gases when the flow rate of  $\text{SnCl}_4$  is of the same order of  $\text{GeH}_4$ .

## OPTICAL CHARACTERIZATION

### Raman spectroscopy

The  $\text{Ge}_{1-x}\text{Sn}_x$  films were further investigated by Raman spectroscopy in order to analyze the crystal structure. Room temperature Raman spectra of the grown samples as well as a Ge reference sample are plotted in **Figure 4A**. The Ge–Ge longitudinal optical (LO) peak was observed at  $300\text{ cm}^{-1}$  for the Ge reference sample while the Ge–Ge peak in the  $\text{Ge}_{1-x}\text{Sn}_x$  films was shifted to lower





wavenumbers due to the change in bonding energy of Ge–Ge by incorporation of Sn atoms. The intensity of the Ge–Ge LO peak at  $300\text{ cm}^{-1}$  is normalized for all the samples for comparison of the peak positions. In addition to the main Ge–Ge peak, Raman spectra of  $\text{Ge}_{1-x}\text{Sn}_x$  films show other peaks that are induced as a result of Sn incorporation. The Ge–Sn LO peaks for different Sn mole fractions were observed at  $250\text{--}260\text{ cm}^{-1}$  in the films. A second peak of Ge–Sn is observed at  $285\text{ cm}^{-1}$ , which can be seen as a shoulder of Ge–Ge main peak.

The peak positions are obtained by Lorentzian fitting to find the exact position for further analysis. The shift in the Ge–Ge LO peak depends on both strain and Sn composition of the films. Theoretical calculations for  $\Delta\omega$  are different for strain-relaxed films and strained films for different Sn ( $x$ ) content [ $\Delta\omega_{\text{Ge-Ge}}(x) = bx\text{ cm}^{-1}$ ]. The Ge–Ge peak is expected to shift by a factor of  $b = -30.30$  for a strained alloy while this factor varies to  $b = -83.10$  for a strain-relaxed film (Cheng et al., 2013). **Figure 4B** shows the experimental data obtained for Ge–Ge and Ge–Sn Raman shift from the sample compared with the theoretical calculations. The peak shifts match well with the theoretical calculations for strain-relaxed films.

### Photoluminescence

Germanium has an indirect band-gap in the L valley with the energy of  $0.644\text{ eV}$  and a direct band-gap at the  $\gamma$  point with  $0.8\text{ eV}$  energy at room temperature. Incorporation of Sn in Ge lattice lowers the conduction band edge at the  $\gamma$ -point at a faster rate than that at the L-point. PL measurements on  $\text{Ge}_{1-x}\text{Sn}_x$  samples allow determination of the band-gap edge for various Sn compositions.

**Figure 5** depicts room temperature PL intensity spectra for as-grown  $\text{Ge}_{1-x}\text{Sn}_x$  films with 2, 4, 6, and 7% Sn mole fractions. As indicated in **Figure 5A**, increase of the Sn mole fraction results in a band-gap reduction. Both direct and indirect PL peaks exhibit red-shift with Sn compositions increase from 2 to 7%. A Gaussian fitting function was employed to extract the PL peak positions of both direct and indirect transitions as described in

Ghetmiri et al. (2014b). In  $\text{Ge}_{0.94}\text{Sn}_{0.06}$  and  $\text{Ge}_{0.93}\text{Sn}_{0.07}$  samples, the energies difference between direct and indirect transitions are very small, therefore the PL emissions from these indirect and direct transitions cannot be identified. A temperature-dependent study is needed to differentiate the direct and indirect peak positions which will be reported in the future. The PL peaks from the samples with 2, 4, 6, and 7% Sn compositions are shown in **Figure 5B** as solid symbols. The solid and the dashed lines show the direct and indirect band-gap energies based on bowed Vegard's law for the relaxed  $\text{Ge}_{1-x}\text{Sn}_x$  alloy (Ghetmiri et al., 2014b), respectively. Since the  $\text{Ge}_{1-x}\text{Sn}_x$  films are almost strain-free, as confirmed by XRD measurements, the experimental results closely follow the predicted values from Vegard's law.

### CONCLUSION

Direct growth of  $\text{Ge}_{1-x}\text{Sn}_x$  layers on Si substrates was achieved using a cold-wall UHV-CVD system. The films were grown by employing low-cost commercial available  $\text{GeH}_4$  and  $\text{SnCl}_4$  precursors without using any carrier gases and buffer layers. Characterizations of the samples with XRD showed successful incorporation of Sn up to 7%. The TEM images show fully epitaxial growth of the samples without any precipitation of Sn from the Ge lattice. The Raman results verified the Sn incorporation and PL measurements showed reduction of the band-gap to  $0.55\text{ eV}$  for 7% Sn sample. The low-cost and CMOS compatible growth method and the performance of the samples indicate a promising future for  $\text{Ge}_{1-x}\text{Sn}_x$  applications in Si photonics. Moreover, the samples were grown strain-relaxed enabling this material to be a universal compliant buffer layer which can be used in hybrid integration.

### ACKNOWLEDGMENTS

The work at the UA was supported by NSF (EPS-1003970), the Arkansas Bioscience Institute, the Arktonics, LLC (Air Force SBIR, FA9550-14-C-0044, Dr. Gernot Pomrenke, Program Manager), and DARPA (W911NF-13-1-0196, Dr. Dev Palmer, Program Manager). Drs. RS and GS acknowledge support from AFOSR

(FA9550-14-1-0196, Dr. Gernot Pomrenke, Program Manager). JG acknowledges the support of NSF REU Program under Grant number EEC-1359306.

## REFERENCES

- Beeler, R. T., Grzybowski, G. J., Roucka, R., Jiang, L., Mathews, J., Smith, D. J., et al. (2011a). Synthesis and materials properties of Sn/P-doped Ge on Si (100): photoluminescence and prototype devices. *Chem. Mater.* 23, 4480–4486. doi:10.1021/cm201648x
- Beeler, R., Roucka, R., Chizmeshya, A., Kouvetakis, J., and Menéndez, J. (2011b). Nonlinear structure-composition relationships in the  $\text{Ge}_{1-y}\text{Sn}_y\text{Si}$  (100) ( $y < 0.15$ ) system. *Phys. Rev. B* 84, 035204. doi:10.1103/PhysRevB.84.035204
- Bhargava, N., Coppinger, M., Gupta, J. P., Wielunski, L., and Kolodzey, J. (2013). Lattice constant and substitutional composition of GeSn alloys grown by molecular beam epitaxy. *Appl. Phys. Lett.* 103, 041908. doi:10.1063/1.4816660
- Bogumilowicz, Y., Hartmann, J. M., Truche, R., Campidelli, Y., Rolland, G., and Bilon, T. (2005). Chemical vapour etching of Si, SiGe and Ge with HCl; applications to the formation of thin relaxed SiGe buffers and to the revelation of threading dislocations. *Semicond. Sci. Technol.* 20, 127. doi:10.1088/0268-1242/20/2/004
- Chen, R., Huang, Y., Gupta, S., Lin, A. C., Sanchez, E., Kim, Y., et al. (2013). Material characterization of high Sn-content, compressively-strained GeSn epitaxial films after rapid thermal processing. *J. Cryst. Growth* 365, 29–34. doi:10.1016/j.jcrysgro.2012.12.014
- Chen, R., Lin, H., Huo, Y., Hitzman, C., Kamins, T. I., and Harris, J. S. (2011). Increased photoluminescence of strain-reduced, high-Sn composition  $\text{Ge}_{1-x}\text{Sn}_x$  alloys grown by molecular beam epitaxy. *Appl. Phys. Lett.* 99, 181125. doi:10.1063/1.3658632
- Cheng, R., Wang, W., Gong, X., Sun, L., Guo, P., Hu, H., et al. (2013). Relaxed and strained patterned germanium-tin structures: a Raman scattering study. *ECS J. Solid State Sci. Technol.* 2, 138–145. doi:10.1149/2.013304jss
- Conley, B. R., Mosleh, A., Ghetmiri, S. A., Du, W., Soref, R. A., Sun, G., et al. (2014a). Temperature dependent spectral response and detectivity of GeSn photoconductors on silicon for short wave infrared detection. *Opt. Express* 22, 15639–15652. doi:10.1364/OE.22.015639
- Conley, B. R., Margetis, J., Du, W., Tran, H., Mosleh, A., Ghetmiri, S. A., et al. (2014b). Si based GeSn photoconductors with a 1.63 A/W peak responsivity and a 2.4  $\mu\text{m}$  long-wavelength cutoff. *Appl. Phys. Lett.* 105, 221117. doi:10.1063/1.4903540
- Du, W., Zhou, Y., Ghetmiri, S. A., Mosleh, A., Conley, B. R., Nazzal, A., et al. (2014a). Room-temperature electroluminescence from  $\text{Ge}/\text{Ge}_{1-x}\text{Sn}_x/\text{Ge}$  diodes on Si substrates. *Appl. Phys. Lett.* 104, 241110. doi:10.1063/1.4884380
- Du, W., Ghetmiri, S. A., Conley, B. R., Mosleh, A., Nazzal, A., Soref, R. A., et al. (2014b). Competition of optical transitions between direct and indirect bandgaps in  $\text{Ge}_{1-x}\text{Sn}_x$ . *Appl. Phys. Lett.* 105, 051104. doi:10.1063/1.4892302
- Ghetmiri, S. A., Du, W., Margetis, J., Mosleh, A., Cousar, L., Conley, B. R., et al. (2014a). Direct-bandgap GeSn grown on Silicon with 2230 nm photoluminescence. *Appl. Phys. Lett.* 105, 151109. doi:10.1063/1.4898597
- Ghetmiri, S. A., Du, W., Conley, B. R., Mosleh, A., Naseem, H. A., Yu, S., et al. (2014b). Shortwave-infrared photoluminescence from  $\text{Ge}_{1-x}\text{Sn}_x$  thin films on silicon. *J. Vac. Sci. Technol. B* 32, 060601. doi:10.1116/1.4897917
- Gurdal, O., Desjardins, P., Carlsson, J., Taylor, N., Radamson, H., Sundgren, J., et al. (1998). Low-temperature growth and critical epitaxial thicknesses of fully strained metastable  $\text{Ge}_{1-x}\text{Sn}_x$  ( $x \leq 0.26$ ) alloys on Ge (001)  $2 \times 1$ . *J. Appl. Phys.* 83, 162–170. doi:10.1063/1.366690
- Kouvetakis, J., and Chizmeshya, A. V. G. (2007). New classes of Si-based photonic materials and device architectures via designer molecular routes. *J. Mater. Chem.* 17, 1649–1655. doi:10.1039/b618416b
- Kouvetakis, J., Menendez, J., and Soref, R. A. *Strain-Engineered Direct-Gap Ge/Sn<sub>x</sub>Ge<sub>1-x</sub> Heterodiode and Multi-Quantum-Well Photodetectors, Laser, Emitters and Modulators Grown on Sn/SiGe<sub>1-y-z</sub> Buffered Silicon*. United States patent US 6897471 B1 (2005).
- Li, H., Brouillet, J., Salas, A., Chaffin, I., Wang, X., and Liu, J. (2014). Low temperature geometrically confined growth of pseudo single crystalline GeSn on amorphous layers for advanced optoelectronics. *ECS Trans.* 64, 819–827. doi:10.1149/06406.0819ecst
- Margetis, J., Ghetmiri, S. A., Du, W., Conley, B. R., Mosleh, A., Soref, R., et al. (2014). Growth and characterization of epitaxial  $\text{Ge}_{1-x}\text{Sn}_x$  alloys and heterostructures using a commercial CVD system. *ECS Trans.* 64, 1830–1830. doi:10.1149/06406.0711ecst
- Moontragoon, P., Soref, R., and Ikonc, Z. (2012). The direct and indirect bandgaps of unstrained  $\text{Si}_x\text{Ge}_{1-xy}\text{Sn}_y$  and their photonic device applications. *J. Appl. Phys.* 112, 073106–073106–8. doi:10.1063/1.4757414
- Mosleh, A., Benamara, M., Ghetmiri, S. A., Conley, B. R., Alher, M. A., Du, W., et al. (2014). Investigation on the formation and propagation of defects in GeSn thin films. *ECS Trans.* 64, 1845–1845. doi:10.1149/06406.0895ecst
- Mosleh, A., Ghetmiri, S. A., Conley, B. R., Abu-Safe, H., Waqar, Z., Benamara, M., et al. (2013). “Nucleation-step study of silicon homoepitaxy for low-temperature fabrication of Si solar cells,” in *Photovoltaic Specialists Conference (PVSC), IEEE 39<sup>th</sup>*. Tampa, FL.
- Mosleh, A., Ghetmiri, S. A., Conley, B. R., Hawkrigge, M., Benamara, M., Nazzal, A., et al. (2014a). Material characterization of  $\text{Ge}_{1-x}\text{Sn}_x$  alloys grown by a commercial CVD system for optoelectronic device applications. *J. Electron. Mater.* 43, 938–946. doi:10.1007/s11664-014-3089-2
- Mosleh, A., Ghetmiri, S. A., Conley, B. R., Abu-Safe, H. H., Benamara, M., Waqar, Z., et al. (2014b). Investigation of growth mechanism and role of  $\text{H}_2$  in very low temperature Si epitaxy. *ECS Trans.* 64, 967–975. doi:10.1149/06406.0967ecst
- Oehme, M., Buca, D., Kostecki, K., Wirths, S., Holländer, B., Kasper, E., et al. (2013). Epitaxial growth of highly compressively strained GeSn alloys up to 12.5% Sn. *J. Cryst. Growth* 384, 71–76. doi:10.1016/j.jcrysgro.2013.09.018
- Stefanov, S., Conde, J., Benedetti, A., Serra, C., Werner, J., Oehme, M., et al. (2012). Laser synthesis of germanium tin alloys on virtual germanium. *Appl. Phys. Lett.* 100, 104101. doi:10.1063/1.3692175
- Takeuchi, S., Sakai, A., Yamamoto, K., Nakatsuka, O., Ogawa, M., and Zaima, S. (2007). Growth and structure evaluation of strain-relaxed  $\text{Ge}_{1-x}\text{Sn}$  buffer layers grown on various types of substrates. *Semicond. Sci. Technol.* 22, S231. doi:10.1088/0268-1242/22/1/S54
- Vincent, B., Gencarelli, F., Bender, H., Merckling, C., Douhard, B., Petersen, D. H., et al. (2011). Undoped and in-situ B doped GeSn epitaxial growth on Ge by atmospheric pressure-chemical vapor deposition. *Appl. Phys. Lett.* 99, 152103–152103–3. doi:10.1063/1.3645620
- Wang, L., Su, S., Wang, W., Gong, X., Yang, Y., Guo, P., et al. (2013). Strained germanium-tin (GeSn) p-channel metal-oxide-semiconductor field-effect-transistors (p-MOSFETs) with ammonium sulfide passivation. *Solid State Electron.* 83, 66–70. doi:10.1016/j.sse.2013.01.031
- Werner, J., Oehme, M., Schmid, M., Kaschel, M., Schirmer, A., Kasper, E., et al. (2011). Germanium-tin pin photodetectors integrated on silicon grown by molecular beam epitaxy. *Appl. Phys. Lett.* 98, 061108–061108–3. doi:10.1063/1.3555439
- Wirths, S., Buca, D., Mussler, G., Tiedemann, A., Holländer, B., Bernardy, P., et al. (2013). Reduced pressure CVD growth of Ge and  $\text{Ge}_{1-x}\text{Sn}_x$  alloys. *ECS J. Solid State Sci. Technol.* 2, N99–N102. doi:10.1149/2.006305jss
- Wirths, S., Geiger, R., Scherrer, P., Ikonc, Z., Tiedemann, A. T., Mussler, G., et al. (2014). “Epitaxy and photoluminescence studies of high quality GeSn heterostructures with Sn concentrations up to 13 at.%,” in *11th International Conference on Group IV Photonics 27–29 August*. Paris.

**Conflict of Interest Statement:** The authors declare that the research was conducted in the absence of any commercial or financial relationships that could be construed as a potential conflict of interest.

Received: 28 January 2015; accepted: 23 March 2015; published online: 27 April 2015.

Citation: Mosleh A, Alher MA, Cousar LC, Du W, Ghetmiri SA, Pham T, Grant JM, Sun G, Soref RA, Li B, Naseem HA and Yu S-Q (2015) Direct growth of  $\text{Ge}_{1-x}\text{Sn}_x$  films on Si using a cold-wall ultra-high vacuum chemical-vapor-deposition system. *Front. Mater.* 2:30. doi: 10.3389/fmats.2015.00030

This article was submitted to *Optics and Photonics*, a section of the journal *Frontiers in Materials*.

Copyright © 2015 Mosleh, Alher, Cousar, Du, Ghetmiri, Pham, Grant, Sun, Soref, Li, Naseem and Yu. This is an open-access article distributed under the terms of the Creative Commons Attribution License (CC BY). The use, distribution or reproduction in other forums is permitted, provided the original author(s) or licensor are credited and that the original publication in this journal is cited, in accordance with accepted academic practice. No use, distribution or reproduction is permitted which does not comply with these terms.